Single Atom Adhesion in Optimized Gold Nanojunctions

M. L. Trouwborst,[1] E. H. Huisman,[1] F. L. Bakker,[1] S. J. van der Molen,[2] and B. J. van Wees[1]

[1]*Physics of Nanodevices, Zernike Institute for Advanced Materials, Rijksuniversiteit Groningen, Nijenborgh 4, 9747 AG Groningen, The Netherlands*

[2]*Kamerlingh Onnes Laboratorium, Leiden University, P.O. Box 9504, 2300 RA Leiden, The Netherlands*

(Received 15 November 2007; published 30 April 2008)

We study the interaction between single apex atoms in a metallic contact, using the break junction geometry. By carefully training our samples, we create stable junctions in which no further atomic reorganization takes place. This allows us to study the relation between the so-called jump out of contact (from contact to tunneling regime) and jump to contact (from tunneling to contact regime) in detail. Our data can be fully understood within a relatively simple elastic model, where the elasticity k of the electrodes is the only free parameter. We find $5 < k < 32$ N/m. Furthermore, the interaction between the two apex atoms on both electrodes, observed as a change of slope in the tunneling regime, is accounted for by the same model.

DOI: 10.1103/PhysRevLett.100.175502 PACS numbers: 62.25.−g, 73.63.Rt, 85.35.−p

Many macroscopic phenomena find their origin on the nanoscale, since they are ultimately due to the interaction between single atoms. A good example is formed by friction and wear, which have been studied for centuries, but still inspire fascinating research. For example, several groups have recently explored methods to minimize friction in nanoelectromechanical systems, where no liquid lubricants can be applied [1]. In this Letter, we focus on the ultimate miniaturization of the problem and investigate adhesion and elasticity on the atomic scale.

The interaction between single atoms can be studied by carefully extending a notched metallic wire, while monitoring its conductance G. As the wire is thinned out, G decreases, until its value is dominated by a few atoms forming a constriction [2]. When pulling is continued, an abrupt rupture of the wire is observed (see Fig. 1, points c to d). Upon closing the contacts, a second jump occurs for many metals, including gold (see Fig. 1, points a to b) [3,4]. These jumps are known as the ''jump out of contact'' (JOC) and ''jump to contact'' (JC), respectively. By carefully studying these discontinuities, one can in principle obtain detailed information on the adhesion forces between two single atoms. However, the details of the hysteretic loop in Fig. 1 are still not fully understood. In fact, no relation between the JC and JOC has been observed so far. The reason for this is that the breaking process is generally accompanied by plastic deformation; i.e., the atoms first reorganize before rupture [5]. Therefore, during closing and opening, the electrodes have a different atomic configuration. The most intriguing example of plastic deformation is the formation of atomic chains prior to breaking [6].

Here, we explore junctions in which no plastic deformation occurs during breaking and making of the single atom contact. This is achieved by properly ''training'' each device first. Figure 1 displays G during the opening and closing of a ''trained'' Au wire. Note that the single gold atom conductance is characterized by a value close to the conductance quantum $G_0 = 2e^2/h$. As can be seen from the absence of conductance steps in the contact regime, no atomic reorganization takes place. Moreover, the curves in Fig. 1 are perfectly reproducible for tens of subsequent runs. Being able to exclude plasticity, we infer that the two jumps (JC and JOC) in Fig. 1 are related to the adhesive forces between the single atoms forming the junction. The remarkable reproducibility of the ''trained'' junctions allows us to test a generic potential energy model. In fact, we show that the whole making and breaking process can be fitted by a single fit parameter: the elasticity of the electrodes.

For our study, it is crucial to minimize drift and vibrations in the electrodes during the measurements. This is

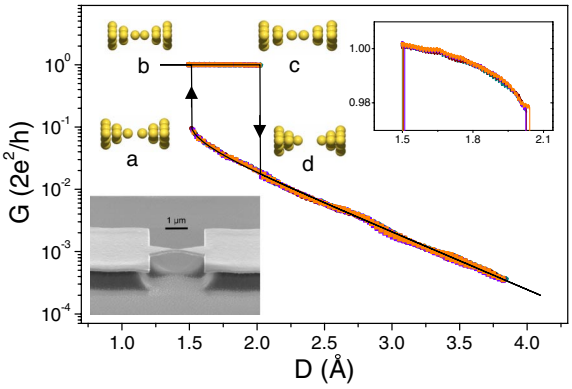

FIG. 1 (color online). Points: conductance G vs distance D for four successive G_0 loops ($V_{\text{bias}} = 50$ mV). The jump to contact occurs at D = 1.5 Å; the jump out of contact at D = 2.0 Å. Black line: fit to model in Fig. 2 ($k = 15.7$ N/m). For the other parameters we use literature values: $F_0 = 1.5$ nN, $d = 2.5$ Å, and $E_b = 0.7$ eV. The work function, $\phi = 5$ eV, was measured independently. Inset graph: zoom of G vs D in contact regime (linear scale). Picture: scanning electron micrograph of a lithographic break junction.

achieved by using a mechanically controllable break junction (MCBJ) at 4.2 K [7]. The wires are patterned with electron beam lithography, after which we evaporate 1 nm of Cr and 120 nm Au at 2×10^{-7} mbar. Finally, the area below the wire is etched with a CF_4/O_2 plasma, to create a free hanging gold wire [inset in Fig. 1]. The MCBJ is cooled down to 4.2 K and broken by bending the substrate. Thus, clean and stable gold electrodes are obtained in cryogenic vacuum. Opening and closing of the junction is done with an effective speed of 0.5 Å/s, while the conductance, at a 50 mV bias, is monitored. Measurements at 1–300 mV gave similar results [8]. We emphasize the impressive stability of the electrodes, resulting in a drift below 0.3 pm/h. Our break junctions are calibrated using Gundlach oscillations [9,10]. We find an attenuation factor $r = (5.4 \pm 0.6) \times 10^{-5}$ [11,12], and a work function $\phi = 5$ eV.

The details of our "training" method are as follows. When closing the electrodes, we stop immediately as soon as the electrodes are in contact, i.e., at $G \approx G_0$, preventing further disorder. Subsequently, we break the wire, extend it 1–2 Å into the tunneling regime and close it again until the jump to contact. Repeating this procedure rearranges and orders the tip atoms. In this way, the atoms are able to probe (energetically and spatially) different positions, allowing them to find the most stable configuration. Remarkably, after typically >10 sweeps, JC and JOC occur at two *exactly* reproducible positions. In Fig. 1, four subsequent traces are shown with perfect repeatability. In fact, the maximum variation in the closing and opening points was less than 5 pm over 50 sweeps. Although these loops (which we call "G_0 loops") have already been observed by other groups [4,13], we are the first to optimize the training method to investigate JC and JOC in well-defined geometries. We have measured 734 different G_0 loops, on 8 different samples, to study the variation in the contacts. To obtain a new G_0 loop, we first rearrange a contact by closing up to $>10G_0$, before training the contact for a different G_0 loop. For each G_0 loop, we automatically record the four conductance values G_a, G_b, G_c, and G_d (at points a, b, c, and d in Fig. 1, respectively). The fact that 85% of the conductance values G_c is above 0.9 G_0 emphasizes the good definition of our junctions. Recently, Untiedt *et al.* studied JC (no "training" method was employed) [14]. A statistical analysis was made of many closing traces and correlations were found between the conductance values just before and just after JC (G_a and G_b). For gold, they observed maxima in density plots, for G_b values below $1G_0$ and around $1.6G_0$. Conductances below $1G_0$ were attributed to a dimer configuration, whereas higher conductances were related to monomer and double bond configurations. We have also observed the peak around $1.6G_0$ for untrained junctions. However, upon breaking G dropped in steps to lower conductances, making it impossible to create stable "G_0 loops" for this configuration. Furthermore, for our trained contacts, more than 80% of our G_b values have a conductance below $1.02G_0$. Therefore, we conclude that training of the contacts results predominantly in the dimer configuration, as sketched in Fig. 1. Also from molecular dynamics simulations, dimers are expected to be the most stable geometry [14,15].

Since for the trained contacts all plastic deformation is removed, we can employ an elastic model to describe the hysteretic loop in Fig. 1. The basic configuration is shown in the inset of Fig. 2, where a dimer is depicted in between two elastic electrodes. To describe the force between the two atoms, we use the so-called "universal" binding curve, which is given by [16–18]

$$E(x) = -\alpha(x - x_0)e^{-\beta(x-x_0)}, \quad (1)$$

where x is the interatomic distance. The parameters α, β, and x_0 are related to the equilibrium bond distance $d = x_0 + 1/\beta$, the binding energy $E_b = -\alpha/\beta e$ and the slope at the inflection point $F_0 = \alpha/e^2$, with $e = 2.718$. These values are known from literature, i.e., $d = 2.5 \pm 0.2$ Å [10], $F_0 = 1.5 \pm 0.3$ nN for the break force [19] and $E_b = 0.7 \pm 0.2$ eV for the binding energy [13]. For the bonding energy of the dimer to the rest of the electrodes (the "banks"), we take the potential energy of a spring $(ku^2/2)$. Hence, we are left with only one free parameter, the spring constant k, which is directly related to the hysteresis of the G_0 loop. In Fig. 2, the total energy is plotted versus the interatomic distance x, for different electrode distances D. Depending on D, two minima are present. When starting with a closed contact in equilibrium, i.e. D = 0 Å, the equilibrium interatomic distance equals $x_{eq} = 2.5$ Å (minimum of curve 1). As the electrodes are pulled apart, e.g., by 1.8 Å (curve 3), the two

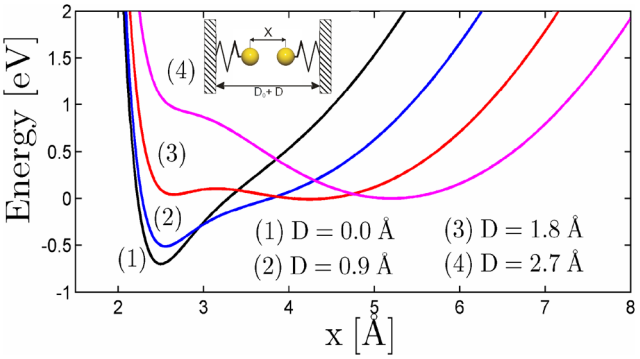

FIG. 2 (color online). Total energy as a function of the interatomic distance x of a gold dimer, for different electrode separations D (see inset; D_0 denotes an offset distance). Two contributions are included: one due to the springs (spring constant k) and one due to the dimer (described by the "universal" binding curve). Depending on D, the total energy may have two minima. For the atom to jump in and out of contact, a barrier has to be overcome. Hence, opening and closing occurs at different positions, explaining the hysteresis in G_0 loops. Note: same parameters as in Fig. 1.

atoms are separated by only 0.2 Å. The rest of the displacement is invested in stretching the spring. Increasing D further (towards curve 4), the first minimum disappears and the system jumps to the second minimum (at $x_{eq} \approx 5.3$ Å); this is JOC. The atoms of the dimer get separated by typically 2–3 Å. Upon closing the junction, a linear relation between x_{eq} and D is initially seen. However, at small separations, the spring stretches somewhat due to the attractive forces of the opposing atoms; i.e., x_{eq} moves faster than D [13,20]. This gives a deviation from exponential tunneling, as observed in Fig. 1. The effect is maximal just before JC, which takes place in between curves 3 and 2, and covers a distance of ≈ 1 Å. To apply our model to the tunneling part of the G_0 loops, we assume that the work function, ϕ, does not depend on x_{eq}, so that $G \propto \exp(-2x_{eq}\sqrt{2m\phi}/\hbar)$. Taking $G = G_0$ for $D = 0$, we have the tools to fit the data in Fig. 1. The corresponding trace is shown in Fig. 1. It gives a perfect fit, not only to the exact position of JC and JOC, but also to the deviation from exponential tunneling. For this G_0 loop, the fit parameter k assumes a value $k = 15.7$ N/m.

In total, we studied $734G_0$ loops, which could all be fitted with the model. In Fig. 3, the conductance G_a (just before JC) is plotted versus G_d (just after JOC), for all G_0 loops measured. Remarkably, the graph shows a relation between these points. This is especially visible in Fig. 3(b), where the average G_a is displayed versus G_d. We compare these data points to our model. By varying the elasticity k from 5–32 N/m, with all other parameters fixed to literature values, one obtains the line drawn in Fig. 3. Clearly, the data points are well described by the model, using only k as a variable. Note that the range of k values is in agreement with Ref. [13]. Moreover, >90% of our k values (per electrode) are in the range 7–26 N/m. This variation is substantially smaller than the spread found in Ref. [13]. We relate the spread in k to the following phenomena. First, breaking a gold wire is only possible along certain crystal orientations ([111], [100], and [110]) [21]. For each orientation, the apex atom is bonded differently to the second layer of the electrode. In fact, the apex atom has 3, 4, and 5 nearest neighbors for the Au [111], [100], and [110] direction, respectively. This is expected to have substantial influence on the elasticity of the electrode. However, this picture is not yet complete. The work by Olesen implies that k is only partly determined by the nearest neighbors of the apex atom [22]. In fact, the most significant contribution to k arises from elastic displacements in the rest of the metal tips. Hence, k is related to the precise structure of the electrodes on a larger scale, which varies with each G_0 loop. Every time we close the junction up to $10G_0$, we most likely introduce defects in the atomic layers further into the contact [23], which influence the elasticity of the electrodes. A final source of variation is the so-called "lateral approach" of the electrodes. For the model in Fig. 2, we assumed that the apex atoms are perfectly aligned. However, small misalignments (0–1 Å) may occur in reality. We extended the 1D model to a 2D model by assuming springs in both x and y directions. This yields a variation in k of up to 10%. We stress that the other parameters in our model cannot explain the data in Fig. 3. Only the spring constant gives a relation along the direction shown. The variation in the vertical direction [Fig. 3(a)], however, can be explained by small deviations in E_b. As indeed shown by Ref. [16], E_b is sensitive to the local atomic configuration. We find that a spread of 25% in E_b explains the variation in G_a. Such a spread is consistent with the results of Ref. [13]. We conclude that our relatively simple model does not only explain the occurrence of JC and JOC, but also their relationship. Finally, we emphasize that without "training," atomic reorganization upon opening and closing destroys the interdependence between G_a and G_d.

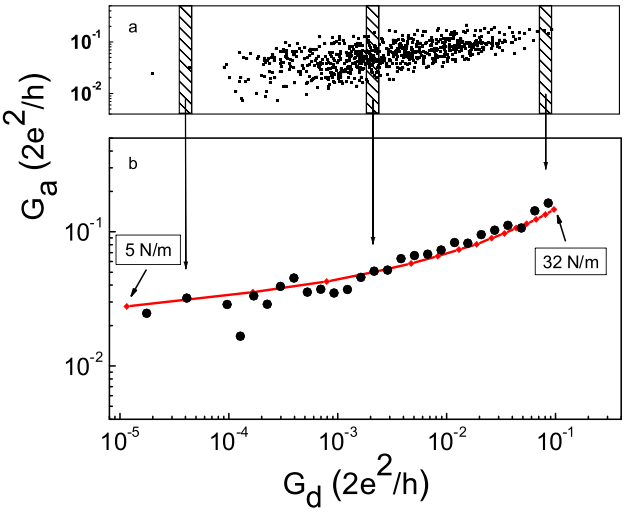

FIG. 3 (color online). (a) Conductance G just before JC (G_a) vs G just after JOC (G_d) for 734 different G_0 loops. (b) Average G_a as a function of G_d. Averaging is done within regular bins of G_d, as indicated in (a). The line is a fit to the model, assuming a varying spring constant $5 < k < 32$ N/m. The other parameters are the same as in Figs. 1 and 2.

Remarkably, our model fits the data in Figs. 1 and 3 very well, despite the fact that we assume a constant barrier height ϕ for all x_{eq}. This contrasts computations by Lang which predict a strong decrease of the apparent barrier at electrode distances <4 Å [24]. Such barrier lowering would primarily be due to the image forces and local effects related to the electric charges on the electrodes. Olesen *et al.* carefully examined the tunnel curves of Ni, Pt, and Au by scanning tunneling microscopy (STM) and found no deviations from exponential behavior. This was explained by assuming that barrier lowering is exactly canceled by adhesion between tip and sample [22]. The fact that we can fit our G_0 loops using an elastic model only, shows that the influence of image forces in break junctions (which feature two sharp tips) is relatively small.

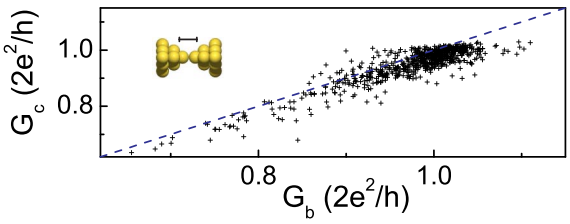

FIG. 4 (color online). (a) Conductance just before JOC (G_c) vs G just after JC (G_b) for 734 different G_0 loops. The dashed line represents $G_c = G_b$. Inset: schematic junction; scale bar: barrier length for tunneling.

Having described three quarters of the G_0 loop (JOC, tunneling and JC), we focus on the contact regime. In Fig. 4, G_c is plotted versus G_b. In all cases, we have $G_c \leq G_0$, as expected for the conductance of a single channel. Furthermore, we find $G_b > G_c$, where on average, G_b is $0.02G_0$ higher than G_c. This is exactly as expected, if a second conductance channel is considered. As calculated by Ref. [15], the small distance between the second layers of the two electrodes allows for tunneling with a conductance of at most $0.03G_0$. When stretching the contact, however, the tunnel gap increases and the transmission of the second channel tends to zero. This is why it is not visible in G_c, where the contact is fully extended. This effect can also be observed in the inset of Fig. 1. Note that the conductance between G_b and G_c decreases nonexponentially, which is a direct consequence of the elasticity of the electrodes.

In summary, we have created highly ordered gold electrodes, using a ''training'' method. Upon opening and limited closing, our junctions show no plastic deformation, allowing us to study the jump out of contact, tunneling curves and jump to contact in detail. Individual breaking and making loops can be perfectly fitted with an elastic model, having the spring constant of the electrodes k as the only free parameter. Hence, by suppressing plastic deformation effects, we are able to measure and model adhesion on the single atomic level.

This work was financed by the Nederlandse Organisatie voor Wetenschappelijk onderzoek, NWO, via a Pionier grant, and the Zernike Institute of Advanced Materials. We thank Simon Vrouwe, Siemon Bakker, and Bernard Wolfs for technical support and Jan van Ruitenbeek for useful discussions.

[1] M. Dienwiebel *et al.*, Phys. Rev. Lett. **92**, 126101 (2004); A. Socoliuc *et al.*, Science **313**, 207 (2006).
[2] N. Agraït, A. Levy-Yeyati, and J. M. van Ruitenbeek, Phys. Rep. **377**, 81 (2003).
[3] J. K. Gimzewski and R. Möller, Phys. Rev. B **36**, 1284 (1987).
[4] J. M. Krans *et al.*, Phys. Rev. B **48**, 14 721 (1993).
[5] G. Rubio, N. Agraït, and S. Vieira, Phys. Rev. Lett. **76**, 2302 (1996).
[6] A. I. Yanson *et al.*, Nature (London) **395**, 783 (1998).
[7] J. Moreland and J. W. Ekin, J. Appl. Phys. **58**, 3888 (1985).
[8] C. Sirvent *et al.*, Physica (Amsterdam) **218B**, 238 (1996).
[9] O. Yu. Kolesnychenko *et al.*, Physica (Amsterdam) **291B**, 246 (2000).
[10] C. Untiedt *et al.*, Phys. Rev. B **66**, 085418 (2002).
[11] S. A. G. Vrouwe *et al.*, Phys. Rev. B **71**, 035313 (2005).
[12] M. L. Trouwborst *et al.* (to be published).
[13] G. Rubio-Bollinger, P. Joyez, and N. Agraït, Phys. Rev. Lett. **93**, 116803 (2004).
[14] C. Untiedt *et al.*, Phys. Rev. Lett. **98**, 206801 (2007).
[15] M. Dreher *et al.*, Phys. Rev. B **72**, 075435 (2005).
[16] S. R. Bahn and K. W. Jacobsen, Phys. Rev. Lett. **87**, 266101 (2001).
[17] J. H. Rose, J. Ferrante, and J. R. Smith, Phys. Rev. Lett. **47**, 675 (1981).
[18] J. M. Krans, Ph.D. thesis, Leiden University, 1996.
[19] G. Rubio-Bollinger *et al.*, Phys. Rev. Lett. **87**, 026101 (2001).
[20] W. A. Hofer *et al.*, Phys. Rev. Lett. **87**, 236104 (2001).
[21] V. Rodrigues, T. Fuhrer, and D. Ugarte, Phys. Rev. Lett. **85**, 4124 (2000).
[22] L. Olesen *et al.*, Phys. Rev. Lett. **76**, 1485 (1996).
[23] I. K. Yanson *et al.*, Phys. Rev. Lett. **95**, 256806 (2005).
[24] N. D. Lang, Phys. Rev. B **37**, 10395 (1988).